

# Stereochemical Control Yields Mucin Mimetic Polymers

Austin G. Kruger,<sup>||</sup> Spencer D. Brucks,<sup>||</sup> Tao Yan, Gerardo Cárcarmo-Oyarce, Yuan Wei, Deborah H. Wen, Dayanne R. Carvalho, Michael J. A. Hore, Katharina Ribbeck, Richard R. Schrock, and Laura L. Kiessling\*



Cite This: *ACS Cent. Sci.* 2021, 7, 624–630



Read Online

ACCESS |



Metrics & More

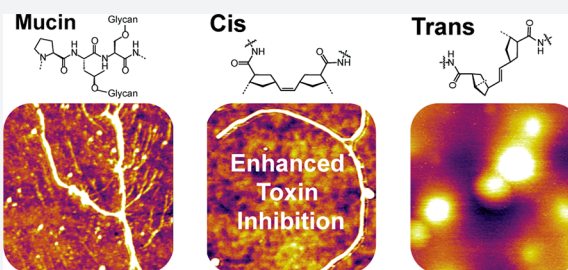


Article Recommendations



Supporting Information

**ABSTRACT:** All animals except sponges produce mucus. Across the animal kingdom, this hydrogel mediates surface wetting, viscosity, and protection against microbes. The primary components of mucus hydrogels are mucins—high molecular weight *O*-glycoproteins that adopt extended linear structures. Glycosylation is integral to mucin function, but other characteristics that give rise to their advantageous biological activities are unknown. We postulated that the extended conformation of mucins is critical for their ability to block microbial virulence phenotypes. To test this hypothesis, we developed synthetic mucin mimics that recapitulate the dense display of glycans and morphology of mucin. We varied the catalyst in a ring-opening metathesis polymerization (ROMP) to generate substituted norbornene-derived glycopolymers containing either *cis*- or *trans*-alkenes. Conformational analysis of the polymers based on allylic strain suggested that *cis*- rather than *trans*-poly(norbornene) glycopolymers would adopt linear structures that mimic mucins. High-resolution atomic force micrographs of our polymers and natively purified Muc2, Muc5AC, and Muc6B mucins revealed that *cis*-polymers adopt extended, mucin-like structures. The *cis*-polymers retained this structure in solution and were more water-soluble than their *trans*-analogs. Consistent with mucin's linear morphology, *cis*-glycopolymers were more potent binders of a bacterial virulence factor, cholera toxin. Our findings highlight the importance of the polymer backbone in mucin surrogate design and underscore the significance of the extended mucin backbone for inhibiting virulence.



## INTRODUCTION

Sponges lack mucus, but all other animals produce it.<sup>1</sup> Mucus coats tissue surfaces, increasing lubrication and providing spatial segregation between a host and its environment.<sup>2</sup> Barrier-forming mucus gels serve as the primary ecological niche for animal microbiomes. Accumulating evidence suggests that while providing this livable habitat mucus barriers can suppress microbial virulence traits.<sup>3–6</sup> In regulating virulence, mucus can trap microbial toxins, act as a shield against microbial invasion, and serve as a food source for symbiotic bacteria.<sup>7–12</sup> These functions are mediated by mucus's primary components, densely glycosylated polypeptides known as mucins. Uncovering the critical attributes of mucins that give rise to these different biological functions has been difficult using genetic or biochemical strategies because mucin biosynthesis is not readily programmable.<sup>13</sup> Synthetic mucin mimics can be readily varied to elucidate what features of these glycoproteins underlie their functional roles. The generation of tailored mucin mimics could lead to a suite of breakthrough technologies, including rewetting materials for eye-care and skin-care, prebiotic dietary supplements, and antibiotic alternatives.<sup>14,15</sup>

Designing mucin surrogates requires an understanding of critical mucin features. As highly *O*-glycosylated proteins, mucins adopt extended linear conformations (Figure 1) that

stretch hundreds of nanometers.<sup>16–26</sup> The resulting viscoelastic properties of mucins have previously been approximated with synthetic mimics, but those agents do not resemble the bottlebrush displays of mucin-linked glycans.<sup>27–31</sup> This glycan presentation is essential to recapitulate because perturbing mucin glycosylation *in vivo* abrogates function.<sup>32–36</sup> Indeed, studies of polymer mimics of mucins highlight the importance of length and glycan identity.<sup>37–39</sup> We postulated that another important attribute of mucins was their extended linear backbones.

To test the role of conformation, we sought to compare the mucin mimicking properties of glycan-substituted polymers that either adopt an extended conformation or a less rigid, globular structure. We reasoned that stereocontrolled ring-opening metathesis polymerization (ROMP) reactions<sup>40–46</sup> would provide access to the target polymers. Though many studies have focused on developing *cis*- or *trans*-selective

Received: November 22, 2020

Published: March 30, 2021





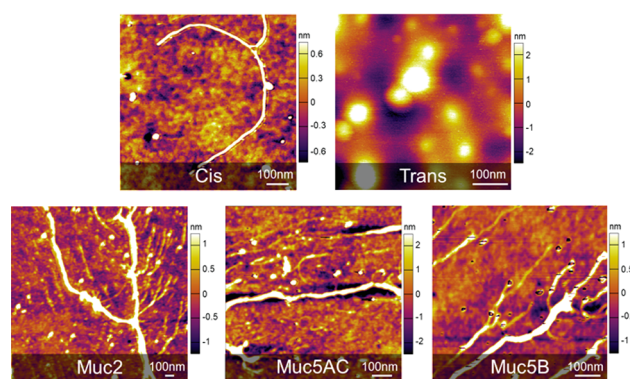


**Figure 3.** Atomic force microscopy images of 50% galactose functionalized cis- and trans-poly(norbornene) 200mers ( $\sim 10$  nM) and natively purified porcine intestinal mucin (Muc2), salivary mucin (Muc5B), and gastric mucin (Muc5AC).

Cis-200mers with 25% galactose functionalization always adopted an extended linear structure (SI Figure 3), but polymers fully substituted with galactose had the most chain entanglement (SI Figure 4). We attribute this behavior to the increased water solubility of the densely glycosylated cis-polymers. During evaporation, highly concentrated droplets form, and their final drying results in the precipitation of clusters of intertangled polymers. By contrast, the trans-polymers always generate spherical globules at both 50% and 100% functionalization densities (SI Figure 5–6). These globules ranged from 10 to 100 nm in diameter and about 4 nm in height, indicating that multiple polymers aggregated.

We next compared the morphology of our synthetic glycopolymers to native secretory mucins. We purified Muc2 (intestinal mucin) and Muc5AC (gastric mucin) from porcine tissue samples, and Muc5B (salivary mucin) from human saliva. Each had a governing morphology corresponding to an extended bottlebrush structure (Figure 3). We imaged the mucin networks over hundreds of nanometers and obtained some of the highest resolution mucin images ever observed. We ascribe these results to the high quality of the isolated mucins, which were carefully purified to ensure minimal degradation and denaturation.<sup>54,55</sup> While all three mucins formed extended, micron-scale bottlebrushes, we also observed a unique condensed morphology in Muc5B (SI Figure 7). Thus, the extended linear structures, exclusively found in the cis-polymer, mimic those of mucins.

To confirm that the morphology observed in the solid-state translated to the solution phase, we analyzed cis- and trans-50%-Gal-200mers by using SANS (Figure 4). SANS enables the determination of the bulk solution structure for polymers composed of light elements. The cis-polymers were best fit to a model of flexible cylinders with a persistence length of 10.5 nm, confirming their solution structure as extended polymer chains. In contrast, trans-polymers, which displayed a steeper slope in their scattering intensity, best fit a globular model with a persistence length of  $\sim 1.6$  nm, indicating that they were coiling in solution. These data indicate cis- and trans-polymers retain the conformations observed in a solid-state in the aqueous phase.

We postulated that the differences in the cis- and trans-poly(norbornene) structures would be relevant for their activity. We evaluated these polymers' relative affinity for the virulence factor cholera toxin (Ctx) and compared them to purified native secretory mucins. *Vibrio cholerae* produce Ctx,

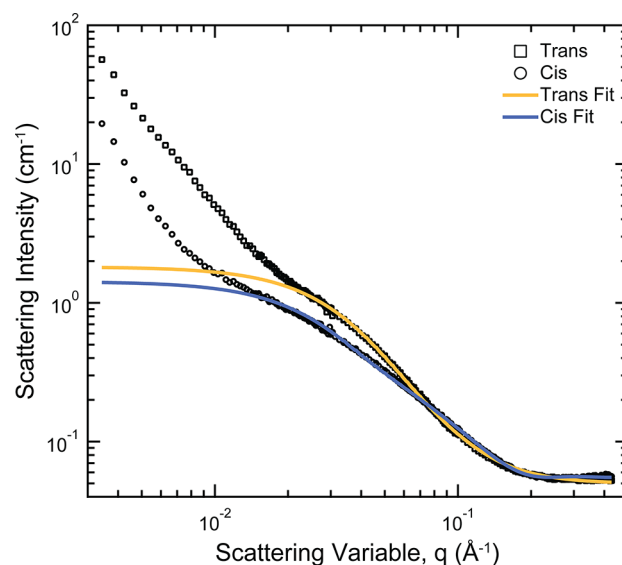


**Figure 4.** Small-angle neutron scattering (SANS) data for 50% galactose-functionalized trans-poly(norbornene) and cis-poly(norbornene) with best-fit lines in yellow and blue, respectively

and the toxin's activity promotes infection. Previous studies suggest that Ctx binding to multivalent galactose derivatives depends on their structure,<sup>51,56</sup> and well-established protocols are available for assaying Ctx inhibitors.<sup>52,56,57</sup> Finally, because Ctx must penetrate the intestinal mucus barrier before it can intoxicate cells, its interaction with mucin-linked galactose is of clinical relevance.<sup>11,58</sup>

We determined the concentration of galactose residues at which half of the toxin was bound ( $IC_{50}$  value) by each polymer (Figure 5).<sup>52</sup> The assay involved exposing fluorescein-labeled Ctx to a dilution series of polymer or mucin and adding the resulting mixtures to a plate coated with the naturally occurring ligand, GM1 ganglioside. Fluorescence was quantified, and the extent of either polymer or mucin binding was assessed in a competition assay. A comparison of the 200mers indicated that the linear cis-polymers had  $IC_{50}$  values 5- to 10-fold lower than those obtained for the corresponding globular trans-polymers. These data indicate a significant preference for cis-polymer binding (Figure 5A). The trans-polymers with galactose residue substitution below 50% were not sufficiently soluble to obtain an  $IC_{50}$  value. In contrast, the cis-analogs were not only soluble but also the best inhibitors tested. Indeed, all cis-materials proved more soluble in aqueous buffer than their trans-counterparts (SI Table 5). The observed binding enhancement for polymers with decreased functionalization is consistent with previous studies on glycan–lectin interactions; this effect presumably arises because high substitution levels result in steric occlusion of epitopes.<sup>51,59</sup> The longer 500mer polymers showed similar trends in Ctx binding and solubility (SI Figure 8).

We similarly tested samples of Muc2, Muc5AC, and Muc5B for Ctx inhibition. As all three mucins are densely glycosylated with an unknown percentage of galactose, an exact galactose concentration could not be established. Instead, we determined the  $IC_{50}$  value as a function of weight percentage and compared those values to the measured inhibition of monomeric D-galactose ( $IC_{50} = 310$  mM and 5.3 wt %) to yield a relative potency (Figure 5B). Select mucins inhibit Ctx, with Muc5B as the most potent. These data suggest that

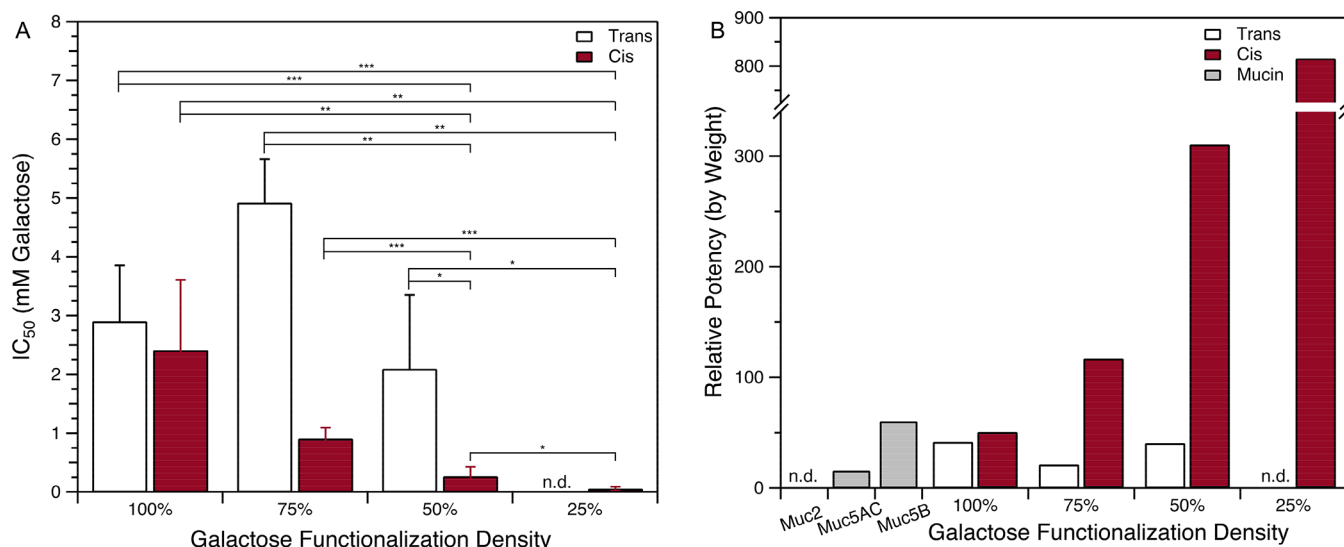


**Figure 5.** (A) Inhibition of cholera toxin binding to GM1 ganglioside by galactose-substituted cis- and trans-poly(norbornene) 200mers. Polymers are listed by their percent galactose functionalization. Inhibition data are reported as the concentration of polymer with respect to galactose at which cholera toxin binding to the GM1 ganglioside was reduced to half of its maximum value ( $IC_{50}$ ). Error bars are the standard deviation of triplicate measurements. \* $P < 0.15$ ; \*\* $P < 0.10$ ; \*\*\* $P < 0.05$ . (B) Relative inhibitory potency toward cholera toxin by weight percent for galactose-functionalized cis- and trans-poly(norbornene) 200mers, Muc2, Muc5AC, and Muc5B relative to monomeric galactose. Values were not determined (n.d.) for those polymers with  $IC_{50}$  values greater than their maximum solubility in buffer.

purified gastric mucin (Muc5AC) and salivary mucin (Muc5B) can serve as efficient decoy receptors for Ctx. Given Muc5B is also highly expressed in the gastrointestinal tract, its mitigating activity may be especially relevant as Ctx acts on intestinal barriers. However, when compared to our synthetic mucin mimics, the native mucins are far less potent inhibitors. This preferential binding of our mucin mimetic polymers is rooted in their design: they have terminal galactose residues for Ctx binding, whereas native mucins possess a diversity of glycans.

We next evaluated whether the observed Ctx binding was galactose-dependent, as we postulated that the observed differences in solubility were due to polymer architecture. To this end, we generated glucamine-functionalized poly(norbornene). Glucamine is an open-chain, reduced sugar that should exhibit no affinity for Ctx. Neither cis- nor trans-glucamine polymer bound to Ctx. As with the galactose-substituted polymers, the cis-polymer was much more water-soluble than its trans-analog (SI Table 5). Together with the Ctx inhibition results, these data indicate that the glycopolymer backbone modulates structure and solubility and can impact glycan–lectin binding in mucin-mimetic interactions.

To assess whether the backbone drives poly(norbornene) conformation and therefore influences Ctx inhibition, we used hydrogenation and syn-dihydroxylation (Figure 6A) to modify the backbone alkenes. Backbone reduction should increase chain flexibility and thereby promote aggregation and enhance globule formation. To test this idea, we subjected our polymers to transfer hydrogenation conditions using *p*-toluenesulfonylhydrazide (Figure 6A, left).<sup>60</sup> The reduction of partially functionalized materials yielded insoluble films, but a fully functionalized galactose 200mer underwent reduction with ~85% efficiency. The resulting polymer was slightly less soluble than its trans-alkene analog and proved to be an equivalent Ctx inhibitor (Figure 6B, left). This finding was unsurprising since differences in inhibition between cis- and trans-polymers are only observed at lower saccharide functionalization densities. Consistent with our structural

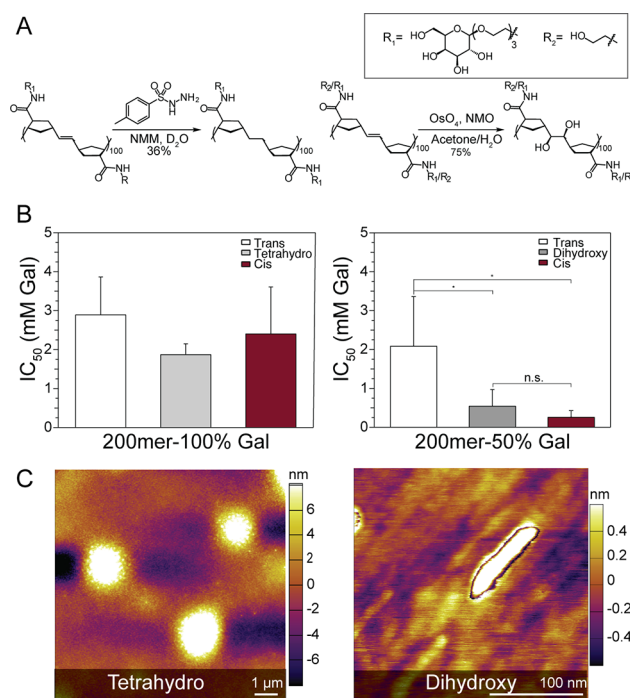


**Figure 6.** (A) Synthetic scheme; (B)  $IC_{50}$  values for cholera toxin; and (C) atomic force microscopy images of galactose-substituted polymers with reduced (left) or dihydroxylated (right) poly(norbornene) backbones. Error bars are the standard deviation of triplicate measurement (for reduced polymers (left) no statistically relevant differences were observed). \* $P < 0.15$ ; n.s.  $P \geq 0.15$ .

prediction, AFM revealed that the polymer with the reduced backbone adopts giant globular structures  $>1 \mu\text{m}$  in diameter (Figure 6C, left).

We compared the results with the fully reduced polymer to those with dihydroxylated polymer. We expected the latter to be less hydrophobic than the parent trans-polymer. Because

the gauche effect should restrict rotational freedom, we anticipated that syn-dihydroxylation would afford materials with a more cis-like morphology, solubility, and potency toward Ctx. Trans-200mers 50% functionalized with galactose readily underwent near quantitative dihydroxylation with osmium tetroxide and *N*-methylmorpholine *N*-oxide (Figure 6A, right). In line with our predictions, the dihydroxy-polymer was far more water-soluble than its parent polymer (SI Table 6). This material yielded an IC<sub>50</sub> value between that of the cis- and trans-polymers (Figure 6B, right) and adopted a compact cylindrical structure intermediate between the morphology of the trans- and cis-polymers (Figure 6C, right). These data suggest that trans-polymer aggregation contributed to their weak affinity for Ctx. Thus, chemical and stereochemical manipulation of poly(norbornene) backbones dramatically affects polymer structure and biological function.

In sum, we synthesized cis-, trans-, dihydroxy-, and tetrahydro-poly(norbornene) functionalized with galactose to evaluate their mucin mimetic properties. We found that the conformation and aggregation states of these poly(norbornene) systems are governed by polymer backbone allylic strain and hydrophobic interactions. Exploiting these structural control elements, we generated cis- and dihydroxy-poly(norbornene), which adopt an extended linear morphology that mimics native mucin. These extended-backbone polymers have enhanced water solubility and more effectively sequester a microbial virulence factor. Our findings outline a critical design principle for synthetic mucin mimics that will guide future studies of mucin's role in microbial symbiosis and pathogenesis and serve as a blueprint for generating mucin mimics that act as lubricants or control microbiome composition and infectious disease.

## ■ ASSOCIATED CONTENT

### SI Supporting Information

The Supporting Information is available free of charge at <https://pubs.acs.org/doi/10.1021/acscentsci.0c01569>.

Experimental procedures, materials, instrumentation, and additional tables and figures including ligand and polymer syntheses, fluorescence inhibition assay protocol, polymer solubility data, Fourier-transform infrared spectroscopy, additional atomic force micrographs, fluorescence inhibition results of 500mers, and <sup>1</sup>H NMR spectra (PDF)

## ■ AUTHOR INFORMATION

### Corresponding Author

Laura L. Kiessling – Department of Chemistry, Massachusetts Institute of Technology, Cambridge, Massachusetts 02139, United States; [orcid.org/0000-0001-6829-1500](https://orcid.org/0000-0001-6829-1500);  
Email: [Kiesslin@mit.edu](mailto:Kiesslin@mit.edu)

### Authors

Austin G. Kruger – Department of Chemistry, Massachusetts Institute of Technology, Cambridge, Massachusetts 02139, United States

Spencer D. Brucks – Department of Chemistry, Massachusetts Institute of Technology, Cambridge, Massachusetts 02139, United States

Tao Yan – Department of Chemistry, Massachusetts Institute of Technology, Cambridge, Massachusetts 02139, United States

Gerardo Cárcarmo-Oyarce – Department of Biological Engineering, Massachusetts Institute of Technology, Cambridge, Massachusetts 02139, United States

Yuan Wei – Department of Macromolecular Science and Engineering, Case Western Reserve University, Cleveland, Ohio 44106, United States

Deborah H. Wen – Department of Chemistry, Massachusetts Institute of Technology, Cambridge, Massachusetts 02139, United States

Dayanne R. Carvalho – Department of Chemistry, Massachusetts Institute of Technology, Cambridge, Massachusetts 02139, United States

Michael J. A. Hore – Department of Macromolecular Science and Engineering, Case Western Reserve University, Cleveland, Ohio 44106, United States

Katharina Ribbeck – Department of Biological Engineering, Massachusetts Institute of Technology, Cambridge, Massachusetts 02139, United States; [orcid.org/0000-0001-8260-338X](https://orcid.org/0000-0001-8260-338X)

Richard R. Schrock – Department of Chemistry, Massachusetts Institute of Technology, Cambridge, Massachusetts 02139, United States; [orcid.org/0000-0001-5827-3552](https://orcid.org/0000-0001-5827-3552)

Complete contact information is available at:  
<https://pubs.acs.org/doi/10.1021/acscentsci.0c01569>

### Author Contributions

||A.G.K. and S.D.B. contributed equally. A.G.K., S.D.B., and L.L.K. conceived of the experimental design. A.G.K., S.D.B., D.H.W., and D.R.C. synthesized and characterized all materials except catalyst 2 and performed atomic force microscopy. G.C.-O. and K.R. provided mucin. Y.W. and M.J.A.H. performed small-angle neutron scattering and interpreted the data. T.Y. and R.R.S. provided catalyst 2. L.L.K. oversaw the majority of the experimental work. A.G.K. and S.D.B. wrote the manuscript with input from all of the authors.

### Funding

This work was funded in part by a Bose research grant through MIT (K.R. and L.L.K.), NIBIB/NIH grant R01 EB017755 (K.R.), National Science Foundation (CHE-1463707) (R.R.S.), and the National Institute of Allergy and Infectious Diseases (AI055258 to L.L.K.).

### Notes

The authors declare no competing financial interest. Protocols involving samples from human participants were approved by the Massachusetts Institute of Technology's Committee on the Use of Humans as Experimental Subjects.

## ■ ACKNOWLEDGMENTS

Dr. Bruce Adams of the MIT Department of Chemistry Instrumentation Facility designed and performed 2D NMR experiments for characterizing polymer alkene geometry. Atomic force microscopy experiments were performed on a Cypher AFM in the Department of Material Science and Engineering's Nanomechanical Technology Laboratory at MIT. We acknowledge the support of the National Institute of Standards and Technology, U.S. Department of Commerce, in providing the neutron research facilities used in this work. Access to the NGB 30 m SANS instrument was provided by the Center for High Resolution Neutron Scattering, a partnership between the National Institute of Standards and

Technology and the National Science Foundation under Agreement No. DMR-2010792.

## ■ ABBREVIATIONS

ROMP, ring-opening metathesis polymerization; AFM, atomic force microscopy; SANS, small-angle neutron scattering; Ctx, cholera toxin

## ■ REFERENCES

- (1) Lang, T.; Klasson, S.; Larsson, E.; Johansson, M. E. V.; Hansson, G. C.; Samuelsson, T. Searching the Evolutionary Origin of Epithelial Mucus Protein Components—Mucins and FCGBP. *Mol. Biol. Evol.* **2016**, *33* (8), 1921–1936.
- (2) Lai, S. K.; Wang, Y.-Y.; Wirtz, D.; Hanes, J. Micro- and Macro-rheology of Mucus. *Adv. Drug Delivery Rev.* **2009**, *61* (2), 86–100.
- (3) Frenkel, E. S.; Ribbeck, K. Salivary Mucins Protect Surfaces from Colonization by Cariogenic Bacteria. *Appl. Environ. Microbiol.* **2015**, *81* (1), 332–338.
- (4) Kavanaugh, N. L.; Zhang, A. Q.; Nobile, C. J.; Johnson, A. D.; Ribbeck, K. Mucins Suppress Virulence Traits of *Candida Albicans*. *mBio* **2014**, *5* (6), No. e01911.
- (5) Caldara, M.; Friedlander, R. S.; Kavanaugh, N. L.; Aizenberg, J.; Foster, K. R.; Ribbeck, K. Mucin Biopolymers Prevent Bacterial Aggregation by Retaining Cells in the Free-Swimming State. *Curr. Biol.* **2012**, *22* (24), 2325–2330.
- (6) Frenkel, E. S.; Ribbeck, K. Salivary Mucins Promote the Coexistence of Competing Oral Bacterial Species. *ISME J.* **2017**, *11* (5), 1286–1290.
- (7) Tailford, L. E.; Crost, E. H.; Kavanaugh, D.; Juge, N. Mucin Glycan Foraging in the Human Gut Microbiome. *Front. Genet.* **2015**, DOI: 10.3389/fgene.2015.00081.
- (8) Van Herreweghen, F.; De Paepe, K.; Roume, H.; Kerckhof, F.-M.; Van de Wiele, T. Mucin Degradation Niche as a Driver of Microbiome Composition and *Akkermansia Muciniphila* Abundance in a Dynamic Gut Model Is Donor Independent. *FEMS Microbiol. Ecol.* **2018**, DOI: 10.1093/femsec/fiy186.
- (9) Salyers, A. A.; Pajeau, M.; McCarthy, R. E. Importance of Mucopolysaccharides as Substrates for *Bacteroides Thetaiotaomicron* Growing in Intestinal Tracts of Exgermfree Mice. *Appl. Environ. Microbiol.* **1988**, *54* (8), 1970–1976.
- (10) Johansson, M. E. V.; Larsson, J. M. H.; Hansson, G. C. The Two Mucus Layers of Colon Are Organized by the MUC2Mucin, Whereas the Outer Layer Is a Legislator of Host-Microbial Interactions. *Proc. Natl. Acad. Sci. U. S. A.* **2011**, *108* (Supplement 1), 4659–4665.
- (11) Strombeck, D. R.; Harrold, D. Binding of Cholera Toxin to Mucins and Inhibition by Gastric Mucin. *Infect. Immun.* **1974**, *10* (6), 1266–1272.
- (12) Monferran, C. G.; Roth, G. A.; Cumar, F. A. Inhibition of Cholera Toxin Binding to Membrane Receptors by Pig Gastric Mucin-Derived Glycopeptides: Differential Effect Depending on the ABO Blood Group Antigenic Determinants. *Infect. Immun.* **1990**, *58* (12), 3966–3972.
- (13) Varki, A. Biological Roles of Glycans. *Glycobiology* **2017**, *27* (1), 3–49.
- (14) Werlang, C.; Cárcarmo-Oyarce, G.; Ribbeck, K. Engineering Mucus to Study and Influence the Microbiome. *Nat. Rev. Mater.* **2019**, *4*, 134–145.
- (15) Authimoolam, S. P.; Dziubla, T. D. Biopolymeric Mucin and Synthetic Polymer Analogs: Their Structure, Function and Role in Biomedical Applications. *Polymers* **2016**, *8* (3), 71.
- (16) Almutairi, F. M.; Cifre, J.-G. H.; Adams, G. G.; Kök, M. S.; Mackie, A. R.; de la Torre, J. G.; Harding, S. E. Application of Recent Advances in Hydrodynamic Methods for Characterising Mucins in Solution. *Eur. Biophys. J.* **2016**, *45* (1), 45–54.
- (17) Axelsson, M. A. B.; Asker, N.; Hansson, G. C. O-Glycosylated MUC2Monomer and Dimer from LS 174T Cells Are Water-Soluble,

Whereas Larger MUC2 Species Formed Early during Biosynthesis Are Insoluble and Contain Nonreducible Intermolecular Bonds. *J. Biol. Chem.* **1998**, *273* (30), 18864–18870.

(18) Sheehan, J. K.; Kirkham, S.; Howard, M.; Woodman, P.; Kutay, S.; Brazeau, C.; Buckley, J.; Thornton, D. J. Identification of Molecular Intermediates in the Assembly Pathway of the MUC5AC Mucin. *J. Biol. Chem.* **2004**, *279* (15), 15698–15705.

(19) Fritz, T. A.; Hurley, J. H.; Trinh, L.-B.; Shiloach, J.; Tabak, L. A. The Beginnings of Mucin Biosynthesis: The Crystal Structure of UDP-GalNAc:Polypeptide  $\alpha$ -N-Acetylgalactosaminyltransferase-T1. *Proc. Natl. Acad. Sci. U. S. A.* **2004**, *101* (43), 15307–15312.

(20) Holmén Larsson, J. M.; Karlsson, H.; Sjövall, H.; Hansson, G. C. A Complex, but Uniform O-Glycosylation of the Human MUC2Mucin from Colonic Biopsies Analyzed by NanoLC/MSn. *Glycobiology* **2009**, *19* (7), 756–766.

(21) Gerken, T. A.; Owens, C. L.; Pasumarthy, M. Determination of the Site-Specific O-Glycosylation Pattern of the Porcine Submaxillary Mucin Tandem Repeat Glycopeptide: MODEL PROPOSED FOR THE POLYPEPTIDE:GalNAc TRANSFERASE PEPTIDE BINDING SITE. *J. Biol. Chem.* **1997**, *272* (15), 9709–9719.

(22) Gum, J. R.; Byrd, J. C.; Hicks, J. W.; Toribara, N. W.; Lamport, D. T.; Kim, Y. S. Molecular Cloning of Human Intestinal Mucin CDNAs. Sequence Analysis and Evidence for Genetic Polymorphism. *J. Biol. Chem.* **1989**, *264* (11), 6480–6487.

(23) Gum, J. R.; Hicks, J. W.; Toribara, N. W.; Rothe, E. M.; Lagace, R. E.; Kim, Y. S. The Human MUC2 Intestinal Mucin Has Cysteine-Rich Subdomains Located Both Upstream and Downstream of Its Central Repetitive Region. *J. Biol. Chem.* **1992**, *267* (30), 21375–21383.

(24) Hong, Z.; Chasan, B.; Bansil, R.; Turner, B. S.; Bhaskar, K. R.; Afdhal, N. H. Atomic Force Microscopy Reveals Aggregation of Gastric Mucin at Low pH. *Biomacromolecules* **2005**, *6* (6), 3458–3466.

(25) Eckhardt, A. E.; Timpte, C. S.; Abernethy, J. L.; Toumadje, A.; Johnson, W. C.; Hill, R. L. Structural Properties of Porcine Submaxillary Gland Apomucin. *J. Biol. Chem.* **1987**, *262* (23), 11339–11344.

(26) Round, A. N.; Berry, M.; McMaster, T. J.; Corfield, A. P.; Miles, M. J. Glycopolymer Charge Density Determines Conformation in Human Ocular Mucin Gene Products: An Atomic Force Microscope Study. *J. Struct. Biol.* **2004**, *145* (3), 246–253.

(27) Canton, I.; Warren, N. J.; Chahal, A.; Amps, K.; Wood, A.; Weightman, R.; Wang, E.; Moore, H.; Armes, S. P. Mucin-Inspired Thermoresponsive Synthetic Hydrogels Induce Stasis in Human Pluripotent Stem Cells and Human Embryos. *ACS Cent. Sci.* **2016**, *2* (2), 65–74.

(28) Authimoolam, S. P.; Vasilakes, A. L.; Shah, N. M.; Puleo, D. A.; Dziubla, T. D. Synthetic Oral Mucin Mimic from Polymer Micelle Networks. *Biomacromolecules* **2014**, *15* (8), 3099–3111.

(29) Cook, M. T.; Smith, S. L.; Khutoryanskiy, V. V. Novel Glycopolymer Hydrogels as Mucosa-Mimetic Materials to Reduce Animal Testing. *Chem. Commun.* **2015**, *51* (77), 14447–14450.

(30) Käschorf, B. T.; Weber, F.; Petrou, G.; Srivastava, V.; Crouzier, T.; Lieleg, O. Mucin-Inspired Lubrication on Hydrophobic Surfaces. *Biomacromolecules* **2017**, *18* (8), 2454–2462.

(31) Mahalingam, A.; Jay, J. I.; Langheinrich, K.; Shukair, S.; McRaven, M. D.; Rohan, L. C.; Herold, B. C.; Hope, T. J.; Kiser, P. F. Inhibition of the Transport of HIV in Vitro Using a pH-Responsive Synthetic Mucin-like Polymer System. *Biomaterials* **2011**, *32* (33), 8343–8355.

(32) Smith, P. L.; Myers, J. T.; Rogers, C. E.; Zhou, L.; Petryniak, B.; Becker, D. J.; Homeister, J. W.; Lowe, J. B. Conditional Control of Selectin Ligand Expression and Global Fucosylation Events in Mice with a Targeted Mutation at the FX Locus. *J. Cell Biol.* **2002**, *158* (4), 801–815.

(33) Ye, J.; Pan, Q.; Shang, Y.; Wei, X.; Peng, Z.; Chen, W.; Chen, L.; Wang, R. Core 2 Mucin-Type O-Glycan Inhibits EPEC or EHEC O157:H7 Invasion into HT-29 Epithelial Cells. *Gut Pathog.* **2015**, *7* (1), 31.

- (34) Wheeler, K. M.; Cárcamo-Oyarce, G.; Turner, B. S.; Dello-Nolan, S.; Co, J. Y.; Lehoux, S.; Cummings, R. D.; Wozniak, D. J.; Ribbeck, K. Mucin Glycans Attenuate the Virulence of *Pseudomonas Aeruginosa* in Infection. *Nature Microbiology* **2019**, *4*, 2146–2154.
- (35) Fu, J.; Wei, B.; Wen, T.; Johansson, M. E. V.; Liu, X.; Bradford, E.; Thomsson, K. A.; McGee, S.; Mansour, L.; Tong, M.; McDaniel, J. M.; Sferra, T. J.; Turner, J. R.; Chen, H.; Hansson, G. C.; Braun, J.; Xia, L. Loss of Intestinal Core 1-Derived O-Glycans Causes Spontaneous Colitis in Mice. *J. Clin. Invest.* **2011**, *121* (4), 1657–1666.
- (36) Venkatakrishnan, V.; Packer, N. H.; Thaysen-Andersen, M. Host Mucin Glycosylation Plays a Role in Bacterial Adhesion in Lungs of Individuals with Cystic Fibrosis. *Expert Rev. Respir. Med.* **2013**, *7* (5), 553–576.
- (37) Gordon, E. J.; Sanders, W. J.; Kiessling, L. L. Synthetic Ligands Point to Cell Surface Strategies. *Nature* **1998**, *392*, 30–31.
- (38) Mowery, P.; Yang, Z.-Q.; Gordon, E. J.; Dwir, O.; Spencer, A. G.; Alon, R.; Kiessling, L. L. Synthetic Glycoprotein Mimics Inhibit L-Selectin-Mediated Rolling and Promote L-Selectin Shedding. *Chem. Biol.* **2004**, *11* (5), 725–732.
- (39) Paszek, M. J.; Dufort, C. C.; Rossier, O.; Bainer, R.; Mouw, J. K.; Godula, K.; Hudak, J. E.; Lakins, J. N.; Wijekoon, A. C.; Cassereau, L.; Rubashkin, M. G.; Magbanua, M. J.; Thorn, K. S.; Davidson, M. W.; Rugo, H. S.; Park, J. W.; Hammer, D. A.; Giannone, G.; Bertozzi, C. R.; Weaver, V. M. The Cancer Glycocalyx Mechanically Primes Integrin-Mediated Growth and Survival. *Nature* **2014**, *511* (7509), 319–325.
- (40) Delaude, L.; Demonceau, A.; Noels, A. F. Probing the Stereoselectivity of the Ruthenium-Catalyzed Ring-Opening Metathesis Polymerization of Norbornene and Norbornadiene Diesters. *Macromolecules* **2003**, *36* (5), 1446–1456.
- (41) Keitz, B. K.; Fedorov, A.; Grubbs, R. H. Cis-Selective Ring-Opening Metathesis Polymerization with Ruthenium Catalysts. *J. Am. Chem. Soc.* **2012**, *134* (4), 2040–2043.
- (42) Fox, H. H.; Lee, J. K.; Park, L. Y.; Schrock, R. R. Synthesis of Five- and Six-Coordinate Alkylidene Complexes of the Type Mo(CHR)(NAr)[OCMe(CF<sub>3</sub>)<sub>2</sub>]<sub>2</sub>Sx and Their Use as Living ROMP Initiators or Wittig Reagents. *Organometallics* **1993**, *12* (3), 759–768.
- (43) Yan, T.; VenkatRamani, S.; Schrock, R. R.; Müller, P. Synthesis of Tungsten Oxo Alkylidene Biphenolate Complexes and Ring-Opening Metathesis Polymerization of Norbornenes and Norbornadienes. *Organometallics* **2019**, *38* (16), 3144–3150.
- (44) McConville, D. H.; Wolf, J. R.; Schrock, R. R. Synthesis of Chiral Molybdenum ROMP Initiators and All-Cis Highly Tactic Poly(2,3-(R)2norbornadiene) (R = CF<sub>3</sub> or CO<sub>2</sub>Me). *J. Am. Chem. Soc.* **1993**, *115* (10), 4413–4414.
- (45) Oskam, J. H.; Schrock, R. R. Rotational Isomers of Molybdenum(VI) Alkylidene Complexes and Cis/Trans Polymer Structure: Investigations in Ring-Opening Metathesis Polymerization. *J. Am. Chem. Soc.* **1993**, *115* (25), 11831–11845.
- (46) Bazan, G. C.; Khosravi, E.; Schrock, R. R.; Feast, W. J.; Gibson, V. C.; O'Regan, M. B.; Thomas, J. K.; Davis, W. M. Living Ring-Opening Metathesis Polymerization of 2,3-Difunctionalized Norbornadienes by Mo(:CHBu-Tert)(:NC<sub>6</sub>H<sub>3</sub>Pr-Iso<sub>2-2,6</sub>)(OBu-Tert)<sub>2</sub>. *J. Am. Chem. Soc.* **1990**, *112* (23), 8378–8387.
- (47) Mangold, S. L.; Carpenter, R. T.; Kiessling, L. L. Synthesis of Fluorogenic Polymers for Visualizing Cellular Internalization. *Org. Lett.* **2008**, *10* (14), 2997–3000.
- (48) Choi, T. L.; Grubbs, R. H. Controlled Living Ring-Opening-Metathesis Polymerization by a Fast-Initiating Ruthenium Catalyst. *Angew. Chem., Int. Ed.* **2003**, *42* (15), 1743–1746.
- (49) Bennett, N. R.; Zwick, D. B.; Courtney, A. H.; Kiessling, L. L. Multivalent Antigens for Promoting B and T Cell Activation. *ACS Chem. Biol.* **2015**, *10* (8), 1817–1824.
- (50) Rauschenberg, M.; Fritz, E.-C.; Schulz, C.; Kaufmann, T.; Ravoo, B. J. Molecular Recognition of Surface-Immobilized Carbohydrates by a Synthetic Lectin. *Beilstein J. Org. Chem.* **2014**, *10*, 1354–1364.
- (51) Polizzotti, B. D.; Maheshwari, R.; Vinkenborg, J.; Kiick, K. L. Effects of Saccharide Spacing and Chain Extension on Toxin Inhibition by Glycopolypeptides of Well-Defined Architecture. *Macromolecules* **2007**, *40* (20), 7103–7110.
- (52) Richards, S.-J.; Jones, M. W.; Hunaban, M.; Haddleton, D. M.; Gibson, M. I. Probing Bacterial-Toxin Inhibition with Synthetic Glycopolymers Prepared by Tandem Post-Polymerization Modification: Role of Linker Length and Carbohydrate Density. *Angew. Chem., Int. Ed.* **2012**, *51* (31), 7812–7816.
- (53) Odijk, T. The Statistics and Dynamics of Confined or Entangled Stiff Polymers. *Macromolecules* **1983**, *16* (8), 1340–1344.
- (54) Co, J. Y.; Cárcamo-Oyarce, G.; Billings, N.; Wheeler, K. M.; Grindy, S. C.; Holten-Andersen, N.; Ribbeck, K. Mucins Trigger Dispersal of *Pseudomonas Aeruginosa* Biofilms. *npj Biofilms Microbiomes* **2018**, *4* (1), 1–8.
- (55) Wagner, C. E.; Turner, B. S.; Rubinstein, M.; McKinley, G. H.; Ribbeck, K. A Rheological Study of the Association and Dynamics of MUC5AC Gels. *Biomacromolecules* **2017**, *18* (11), 3654–3664.
- (56) Polizzotti, B. D.; Kiick, K. L. Effects of Polymer Structure on the Inhibition of Cholera Toxin by Linear Polypeptide-Based Glycopolymers. *Biomacromolecules* **2006**, *7* (2), 483–490.
- (57) Haksar, D.; de Poel, E.; van Ufford, L. Q.; Bhatia, S.; Haag, R.; Beekman, J.; Pieters, R. J. Strong Inhibition of Cholera Toxin B Subunit by Affordable, Polymer-Based Multivalent Inhibitors. *Bioconjugate Chem.* **2019**, *30* (3), 785–792.
- (58) Sanchez, J.; Holmgren, J. Cholera Toxin—a Foe & a Friend. *Indian J. Med. Res.* **2011**, *133* (2), 153–163.
- (59) Schuster, M. C.; Mortell, K. H.; Hegeman, A. D.; Kiessling, L. L. Neoglycopolymers Produced by Aqueous Ring-Opening Metathesis Polymerization: Decreasing Saccharide Density Increases Activity. *J. Mol. Catal. A: Chem.* **1997**, *116* (1), 209–216.
- (60) Kanai, M.; Mortell, K. H.; Kiessling, L. L. Varying the Size of Multivalent Ligands: The Dependence of Concanavalin A Binding on Neoglycopolymer Length. *J. Am. Chem. Soc.* **1997**, *119* (41), 9931–9932.

#### ■ NOTE ADDED AFTER ASAP PUBLICATION

Published ASAP on March 30, 2021; Revised April 5, 2021 to correct typographical errors in mucin nomenclature.